Acta of Bioengineering and Biomechanics
Vol. 24, No. 2, 2022

Original paper
DOI: 10.37190/ABB-01994-2021-01

Stress analysis of total hip arthroplasty with a fully hydroxyapatite-coated stem: comparing thermoelastic stress analysis and CT-based finite element analysis

RYUNOSUKE WATANABE[1], HAJIME MISHIMA[1]*, HIRONORI TAKEHASHI[1], HIROSHI WADA[1], SHO TOTSUKA[1], TOMOFUMI NISHINO[1], MASASHI YAMAZAKI[1], KOJI HYODO[2]

[1] Department of Orthopaedic Surgery, Faculty of Medicine, University of Tsukuba, Tsukuba, Japan.
[2] Environment and Safety Division, National Institute of Advanced Industrial Science and Technology (AIST).

Purpose: The aim of this study was to evaluate the stress distribution in a synthetic femur that was implanted with a fully hydroxyapatite-coated stem using thermoelastic stress and finite element analyses, and to clarify the differences in the stress distributions between these two methods. *Methods*: Thermoelastic stress analysis is a stress-analysis technique that employs the thermoelastic effect. Sinusoidal vertical loads were applied to the head of the stem placed on the synthetic femur, and surface stress distribution images were acquired using an infrared stress measurement system. The finite element model for the synthetic femur and stem were set up similarly to the thermoelastic stress analysis experiment, and vertical load was applied to the head of the stem. Surface stress distribution and stress values obtained via these two methods were compared. *Results*: Thermoelastic stress analysis showed that compressive and tensile stresses were distributed from the proximal femur to the diaphysis, not only on the medial and lateral surfaces, but also on the anterior and posterior surfaces. However, finite element analysis showed that compressive stress was not distributed on the anterior and posterior surfaces of the femoral intertrochanter. The stress values of thermoelastic stress analysis tended to be higher in the proximal femur than that obtained via the finite element analysis. *Conclusions*: The surface stress distribution obtained by these two methods were different specifically in the proximal femur. Our results imply that thermoelastic stress analysis has a better potential than finite element analysis to show the surface stress distribution that reflects the stem design.

Key words: *total hip arthroplasty, thermoelastic stress analysis, computed tomography-based finite element analysis, fully hydroxyapatite-coated stem, femoral stress distribution*

1. Introduction

Total hip arthroplasty (THA) is one of the most common orthopedic surgeries. THA involves replacing a deformed hip joint with a prosthesis to relieve pain and improve function. Owing to recent improvements in implants and surgical techniques, good long-term results have been reported, and THA is widely performed worldwide. However, some postoperative problems remain, which affect long-term results, such as aseptic loosening, bone atrophy, infection, dislocation and periprosthetic fracture [24]. Moreover, the stress transfer in the femur changes after THA. Stress transfer depends on stem design, size, material, and fixation method (cemented or cementless). Femoral remodeling occurs in response to changes in stress transfer [15], [20]. Among the problems caused by femoral remodeling, bone atrophy of the proximal femur is particularly problematic. Bone atrophy in the proximal femur is caused by stress shielding [9]. Therefore, implant design and stress distribution in the femur

* Corresponding author: Hajime Mishima, Department of Orthopaedic Surgery, Faculty of Medicine, University of Tsukuba. E-mail: hmishima@md.tsukuba.ac.jp
Received: December 1st, 2021
Accepted for publication: April 12th, 2022

after stem insertion have been studied, in attempts to improve stress transfer to the proximal femur.

The strain gauge method is commonly used in conventional studies of femur stress analysis [1], [3], [10], [18], [19], [23]. In this method, the number of gauges is limited and it is difficult to observe the stress distribution over the entire surface of the femur. Computed tomography (CT)-based finite element analysis (FEA) has also been reported as a useful method for evaluating stress distribution in the femur after THA [13], [14], [21], [26]. Although this method has become widely used in recent years due to improvements in computer performance, it is important to validate and evaluate the method with an experimental model; FEA is only a numerical model based on simulation. Hyodo et al. [16] reported on an experimental system to visualize changes in the surface stress distribution of a synthetic femur implanted with a stem in two dimensions using thermoelastic stress analysis (TSA). TSA is a method in which small temperature changes due to the thermoelastic effect of a sample are measured by an infrared camera and converted into the change of the sum of the principal stresses on the sample surface. Because this method can evaluate the stress distribution on the entire surface of a synthetic femur as an image, even small stress distributions that cannot be assessed by conventional methods may be measured.

The fully hydroxyapatite (HA)-coated stem is a cementless stem that has been widely used in recent years with good results [25], [28]. However, there have been few reports of stress analysis using this type of stem. Therefore, the purpose of this study was to evaluate the stress distribution in a synthetic femur that was implanted with a fully HA-coated stem using TSA and CT-based FEA, and to clarify the differences in the stress distributions provided by the two methods.

2. Materials and methods

2.1. Synthetic femur

The synthetic femur (Composite femur® #3403, Pacific Research Laboratories, USA) used in this study was manufactured from glass-filled epoxy. It is made to mimic the mechanical properties and morphology of natural human bone and is constructed from cortical bone and cancellous bone [11], [12]. The thermoelastic properties of the glass-filled epoxy used for cortical bone has a linear relationship between the change in the sum of principal stresses and temperature change. A temperature change of 1 K corresponds to a change in the sum of principal stresses of approximately 227 MP [16] (Fig. 1).

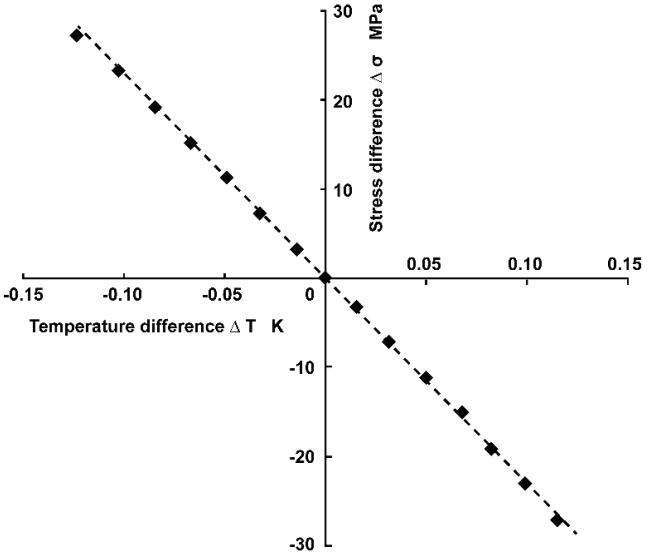

Fig. 1. Thermoelastic property of the synthetic bone [16]

2.2. Stem and head

We used POLARSTEM#0 (Smith & Nephew, USA), a fully HA-coated stem that has been used clinically since 2002 (and used in Japan since 2017). It is made of titanium alloy (Ti-6Al-4V) with a 50 μm HA coating on the surface. The cancellous bone around the stem can be preserved because the compaction rasp compresses the cancellous bone during rasping. The triple-tapered design of the stem is expected to provide initial fixation, rotational stability, and load transfer at the proximal femoral region. A 32-mm diameter OXINIUM femoral head (Smith & Nephew, USA) was used as the head.

2.3. Thermoelastic stress analysis

2.3.1. Thermoelastic stress imaging method

The thermoelastic effect is the change in temperature that accompanies stress change under the adiabatic conditions of a body, as described in Eq. (1), as proposed by Thomson in 1853 [29].

The equation relating temperature changes to applied stress under adiabatic conditions in a linear elastic isotropic homogeneous material is

$$\Delta T = -k \cdot T \cdot \Delta(\sigma_1 + \sigma_2), \qquad (1)$$

where:

ΔT – temperature change [K],

k – thermoelastic constant of the material [1/Pa],

T – absolute temperature of the material [K],

$\Delta(\sigma_1 + \sigma_2)$: sum of principal stresses [Pa].

The thermoelastic constant, k, is given by

$$k = \alpha/\rho\,(\rho \cdot C_p),$$

α – coefficient of linear thermal expansion [K^{-1}],

ρ – density [kg/m^3],

C_p – coefficient of specific heat at constant pressure of the material [J/(kg · K)].

The thermoelastic stress imaging method is based on measurement of a small temperature change (ΔT) that occurs in a material when it is subjected to elastic cyclic loading. The temperature change is converted to the change in the sum of the principal stresses using Eq. (1). It is not possible to measure principal stress components σ_1 and σ_2, separately. A high-precision infrared thermography camera was used for these measurements. This stress-analysis method has been applied in industrial fields as well as skeletal systems [7], [8], [22].

2.3.2. Setting of synthetic femur and stem

The distal part of the synthetic femur was fixed in a specimen holder with bolts and bone cement at the physiological adduction position (9° valgus) in the one-legged stance loading position (Fig. 2). After the synthetic femur was set, the femoral neck was cut and the cancellous bone was rasped with a compaction rasp as in the usual THA surgical method. The POLARSTEM#0 (standard neck, collarless) was then implanted in the femur, and a 32-mm diameter OXINIUM femoral head was attached to the neck of the stem. The surface of the specimen was coated with matte black heat resistant paint (ASAHIPEN Corporation, Japan) to fix surface emissivity.

Fig. 2. Image of the setting of a synthetic femur

2.3.3. Thermoelastic stress measurement

The specimen holder was fixed in the servohydraulic testing machine (Tensilon UTM-10T®, TOYO BOLDWIN, Japan and MiniBionix858; MTS Systems Corporation, USA). The apparatus applied a 5-Hz sinusoidal compressive load of 1.0 ± 0.9 kN to the femoral head through a steel plate. Surface stress distribution images of the femur were acquired in the anterior, posterior, medial, and lateral planes using an infrared stress measurement system (Silver450M 7500; Cedip [FLIR], France) (Fig. 3).

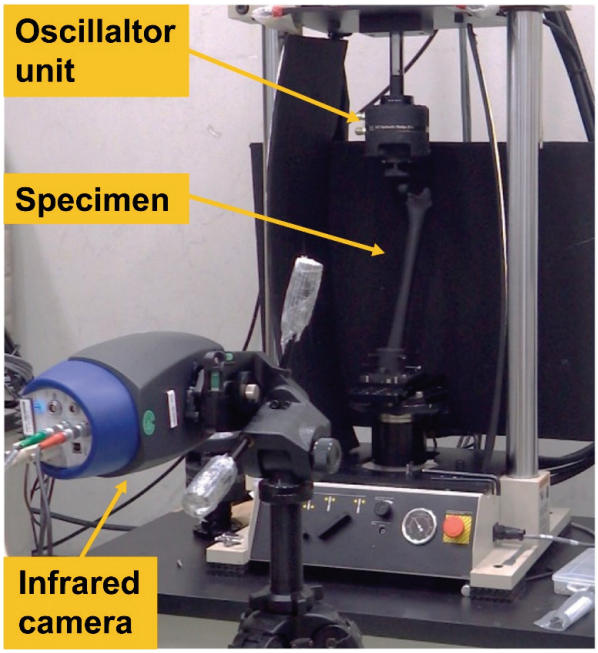

Fig. 3. Thermoelastic stress measurement of a synthetic femur

2.4. CT-based finite element analysis

2.4.1. CT scan

After the synthetic femur was fixed in the specimen holder and implanted with the stem, CT scans (Supria®, Q2J-BW1645-1; Hitachi Medical Corporation, Japan) were performed with a bone mass phantom (QRM-BDC, QRM, Germany) and saved as DICOM

data. The following scanner settings were employed: 1.25 mm slice thickness, 1 mm slice spacing, 20 cm FOV, and 512 × 512 pixel resolution.

2.4.2. Finite element modeling and analysis

A finite element model was constructed and analyzed using the Mechanical Finder ver. 11.0 (Research Center of Computational Mechanics, Japan). First, a model was constructed by extracting only the synthetic femur and specimen pot from the DICOM data. The CAD data from the POLARSTEM was then set in the same position as the stem to construct a model of the synthetic femur and stem. We used 1- to 4-mm four-node tetrahedral solid elements to construct a three-dimensional finite element model for both the synthetic femur and stem, and triangular plate shell elements with a thickness of 0.001 mm were attached to the synthetic femoral surface. The finite element model of the synthetic femur and stem consisted of approximately 320 000 nodes, 1 600 000 elements, and 170 000 shells. The Young's modulus of the synthetic femur was determined using the equations proposed by Keyak et al. [17], according to CT density values. The Poisson's ratio of the synthetic femur was assumed to be 0.4. The Young's modulus and Poisson's ratio of the stem were set to 108 GPa and 0.28, respectively, according to the material property values of Ti-6Al-4V. The head was 32 mm in diameter, and the Young's modulus and Poisson's ratio were set to the material property values of Ti-6Al-4V as those of the stem. The models assumed a completely bonded interface between the stem and the bone. The model was set to 9° valgus, as in the TSA, restrained at the specimen holder, and a compressive vertical load of 1900 N was applied to the femoral head (Fig. 4).

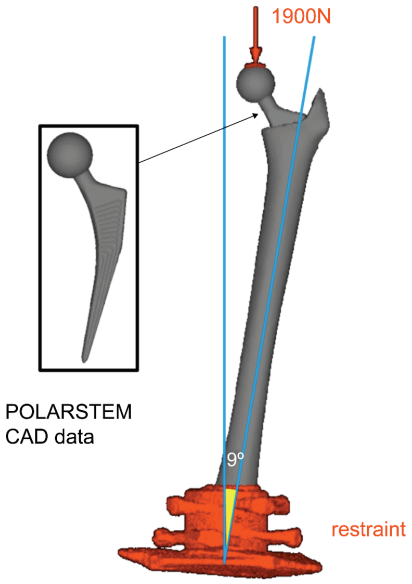

Fig. 4. Setting of a finite element model

2.5. Stress value comparison between TSA and FEA

In the TSA, the change in the sum of the principal stresses for each pixel at the center of the bone axis was plotted. In the FEA, the sum of the principal stress (maximum principal stress + minimum principal stress) for each surface element extracted along the center of the bone axis was plotted. Graphs were made for the anterior, posterior, medial and lateral surfaces, in order to compare the TSA and FEA approaches.

3. Results

3.1. TSA

The change in the sum of the surface principal stresses of the synthetic femur was evaluated. On the medial side of the synthetic femur, compressive stress (warm color) was distributed from the lesser trochanter to the distal side. Tensile stress (cold color) was distributed on the lateral side of the synthetic femur. On both the medial and lateral sides, the stress gradually decreased from proximal to distal. Compressive stress was also distributed on the anterior and posterior surfaces of the femoral intertrochanter (Fig. 5).

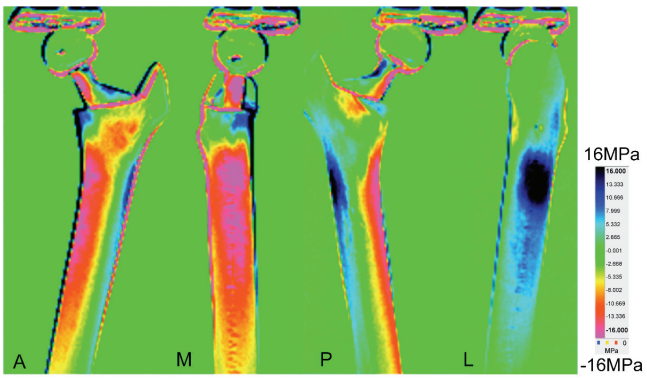

Fig. 5. Results of thermoelastic stress analysis. Anterior (A), medial (M), posterior (P), and lateral (L) views

3.2. CT-based FEA

The surface stress distribution of the synthetic femur was evaluated using a tensor. On the medial side of the synthetic femur, compressive stress (warm color) was distributed from the lesser trochanter to the distal

side. Tensile stress (cold color) was distributed on the lateral side of the synthetic femur. However, compressive stress was not distributed on the anterior and posterior surfaces of the femoral intertrochanter (Fig. 6).

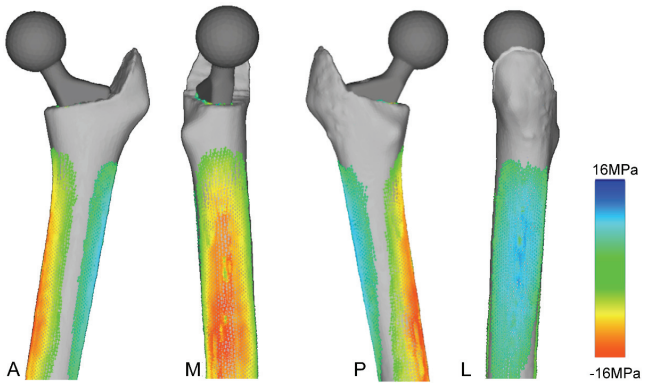

Fig. 6. Results of finite element analysis. Anterior (A), medial (M), posterior (P), and lateral (L) views

3.3. Stress value comparison between TSA and FEA

On the anterior surface, compressive stress was distributed higher in the TSA compared to FEA from the femoral intertrochanter to the diaphysis. On the medial side, compressive stress was distributed higher when analyzed by TSA than by FEA from the lesser trochanter to the level of the center of the stem. From the level of the center of the stem to the diaphysis, a higher compressive stress was distributed in the FEA. On the lateral side, tensile stress was revealed to be distributed higher using TSA than when using FEA from the lesser trochanter to the level of the center of the stem and the medial side (Fig. 7).

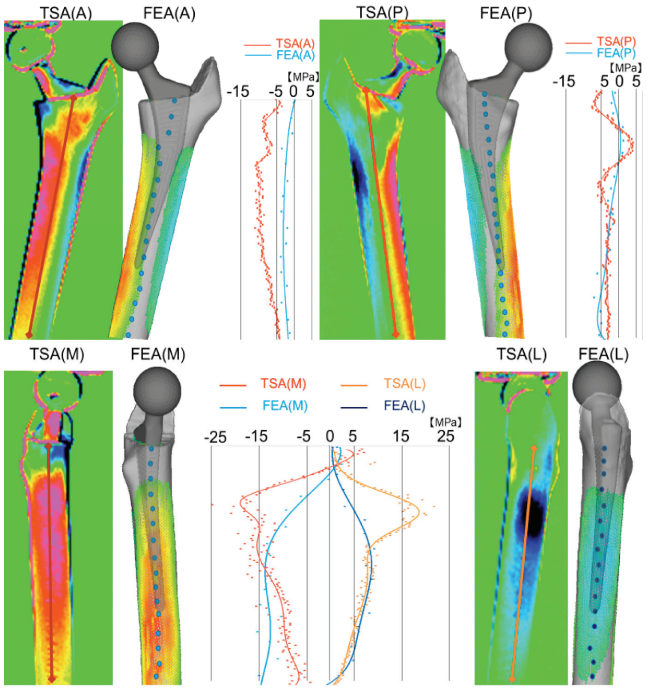

Fig. 7. Comparison of stress values from thermoelastic stress analysis (TSA) and finite element analysis (FEA). The stress value of TSA is the change of the sum of the principal stresses ($\Delta(\sigma_1 + \sigma_2)$). The stress value of FEA is the sum of the principal stress (maximum principal stress + minimum principal stress). A negative stress value indicates compressive stress, and a positive stress value indicates tensile stress. Anterior (A); posterior (P); medial (M); lateral (L)

4. Discussion

In this study, the surface stress distribution of the synthetic femur implanted with POLARSTEM was compared using TSA and CT-based FEA. By TSA, compressive and tensile stresses were distributed from the proximal femur to the diaphysis, not only on the medial and lateral surfaces, but also on the anterior and posterior surfaces. The stress values of TSA tended to be higher in the proximal femur than in the FEA.

The most important feature of the surface stress distribution analysis of the synthetic femur by TSA is that the stress distribution over the entire surface of the synthetic femur can be evaluated without contact, therefore, the usefulness of this analysis method has been reported. A previous study showed that the differences in surface stress distribution due to the type of stem implanted in the synthetic femur and the differences in surface stress distribution due to the use of cement can be visualized using TSA [16]. A different study reported that the effect of the contact site between the stem and the cortical bone on the surface stress distribution can be evaluated using changes in the fine surface stress distribution [27]. Another study reported that the differences in surface distribution due to the head offset installed on stem can be evaluated [7]. In addition, one of the features of this method is that it can evaluate changes in the sum of principal stresses at any point, on any line, or in any region, as can be seen in the current study, which is not possible using the strain gauge method.

The unique feature of fully HA-coated stem is that the cancellous bone is compacted with a compaction rasp prior to stem placement. The purpose of compressing the cancellous bone is to hold the stem with the entire compressed cancellous bone. This technique promotes osseointegration of HA and cancellous bone, resulting in biological fixation of the whole stem. CORAIL (Depuy Synthes, USA) was first used in 1986, and good long-term results with less postop-

erative stress shielding, cortical hypertrophy and thigh pain have been reported [30]. POLARSTEM is one of several fully HA-coated stems that have been in use since 2002. It has a triple-tapered design to transfer the load to the proximal part, improving the initial fixation and preventing stem subsidence. Good mid-term results with a 7-year survival rate of 97.69%, a revision rate of 1.47%, and good long-term results with an 11-year survival rate of 99.1% have been reported [2], [6]. In radiographic analysis, there were no cases of stem subsidence or loosening, and bone atrophy around the stem did not occur in 99% of cases [6], [31].

In this study, the surface stress distribution of the simulated femur determined by TSA showed that high compressive and tensile stresses were distributed from the proximal part, and compressive stress was also distributed on the anterior and posterior surfaces of the femoral intertrochanter. We consider this result to be due to the stress distribution caused by the proximal load transfer of the triple-tapered design of the POLARSTEM, with the compressed cancellous bone around the stem holding up the whole stem. In clinical use, we consider that the high stress distribution proximally leads to good initial fixation without stem subsidence, and to proximal load transfer with less bone atrophy. Furthermore, although many previous studies have examined the stress distribution on the medial and lateral surfaces of the femur, few studies have reported the stress distribution on the anterior and posterior surfaces, especially in the femoral intertrochanter. Although the stress distributions on the anterior and posterior surfaces are smaller than those on the medial and lateral surfaces, we were able to focus on these because TSA may be used to show stress on the entire surface.

Previous studies showed that the correlation between the surface stress distribution shown by TSA and FEA. However, they reported about the surface stress distribution of metal or implant [4], [5]. To the best of the authors' knowledge, currently there are no reports that compare TSA and FEA in terms of surface distribution of synthetic femur with a stem. In this study, differences in stress distribution were observed between TSA and FEA. This difference in stress distribution may be due to the difference in the contact conditions between the stem and bone. In TSA, the stem and bone were not bonded in the experiment. However, in FEA, the stem and bone were analyzed as fully bonded. The stability of the stem immediately after THA using POLARSTEM is fixed by the stem design, surface finish and mechanical stability achieved by the compressed cancellous bone around the stem. This condition is similar to the contact condition between the stem and the synthetic bone in the TSA. Therefore, TSA may be able to evaluate the stress distribution that reflects stem design more accurately than FEA. In the future, it is necessary to investigate whether the stress distribution obtained in this study correlates with radiographic bone remodeling and bone mineral density changes around the stem after THA using POLARSTEM in clinical practice.

This study had several limitations. The first limitation is that the edge effect in TSA causes errors in the change in the sum of principal stresses at the edge of the synthetic femur taken by the infrared camera. The edge effect is a large measurement error caused by the temperature difference between the synthetic femur and the background. This is due to a small displacement of the synthetic femur that is unavoidable in TSA. However, because the stress value of the change in the sum of principal stress was measured at the center of the bone axis of each plane, the error due to the edge effect was negligible. The second limitation is that the DICOM data used for the CT-based FEA were taken after stem implantation, therefore, the CT values of the cancellous bone around the stem may be higher because of metal artifacts around the stem. This limitation could be overcome by simulating FEA using DICOM data of the synthetic bone, wherein the stem was inserted and then removed, which may solve the problem of metal artifacts. The third limitation is the difference in the state of contact between the stem and bone: in FEA, the stem and bone were assumed to be fully bonded, whereas in TSA, the stem and bone were not bonded. To simulate the contact conditions of the TSA in FEA, it was necessary to set the friction coefficient between: the (1) stem and cortical bone, and the (2) stem and cancellous bone. These limitations may have affected the stress distributions observed in this study. However, as the TSA is capable of evaluating the entire surface stress distribution, which can be compared to the FEA, the contact conditions of FEA may be validated by TSA, The validated FE model may be able to evaluate stress distribution under more complex loading conditions that cannot be tested with TSA.

5. Conclusions

In this study, TSA showed that the synthetic femur implanted with POLARSTEM, one of the fully HA-coated stems, was stressed from the proximal part not only on the medial and lateral surfaces, but also on the

anterior and posterior surfaces. Results imply that TSA has a better potential than FEA to visualize the surface stress distribution that reflects the stem design of an entire synthetic femur.

Acknowledgements

Funding: This research received no external funding.

Institutional Review Board Statement: Ethical approval was not required due to the nature of the study.

Informed Consent Statement: Not applicable.

Data Availability Statement: The datasets used and/or analyzed during the current study are available from the corresponding author on reasonable request.

Conflicts of Interest

The authors declare no conflict of interest.

References

[1] AAMODT A., LUND-LARSEN J., EINE J., ANDERSEN E., BENUM P., HUSBY O.S., *Changes in proximal femoral strain after insertion of uncemented standard and customised femoral stems, An experimental study in human femora*, J. Bone Joint Surg. Br., 2001, 83, 921–929.

[2] ASSAF A., MANARA J.R., TEOH K.H., EVANS A.R., *Mid-term clinical results of the cementless R3 cup and Polarstem total hip arthroplasty*, Eur. J. Orthop. Surg. Traumatol., 2019, 29, 827–833.

[3] BIEGER R., IGNATIUS A., DECKING R., CLAES L., REICHEL H., DURSELEN L., *Primary stability and strain distribution of cementless hip stems as a function of implant design*, Clin. Biomech., (Bristol, Avon), 2012, 27, 158–164.

[4] BOUGHERARA H., SALEEM M., SHAH S., TOUBAL L., SARWAR A., SCHEMITSCH E.H., ZDERO R., *Stress analysis of a carbon fiber-reinforced epoxy plate with a hole undergoing tension: A comparison of finite element analysis, strain gages, and infrared thermography*, J. Compos. Mater., 2018, 52 (19), 2679–2689.

[5] CANNELLA F., GARINEI A., D'IMPERIO M., ROSSI G., *A novel method for the design prostheses based on thermoelastic stress analysis and finite element analysis*, J. Mech. Med. Biol., 2014, 14 (5), 1450064.

[6] CYPRES A., FIQUET A., GIRARDIN P., FITCH D., BAUCHU P., BONNARD O., NOYER D., ROY C., *Long-term outcomes of a dual-mobility cup and cementless triple-taper femoral stem combination in total hip replacement: a multicenter retrospective analysis*, J. Orthop. Surg. Res., 2019, 14, 376.

[7] ELISABETTA M.Z., ALBERTO L.A., *Differential thermography for experimental, full-field stress analysis of hip arthroplasty*, J. Mech. Med. Biol., 2010, 10 (3), 515–529.

[8] ELISABETTA M.Z., CRISTINA B., ALBERTO L.A., *Human pelvis loading rig for static and dynamic stress analysis*, Acta Bioeng. Biomech., 2012, 14 (2), 61–66.

[9] ENGH C.A., BOBYN J.D., GLASSMAN A.H., *Porous-coated hip replacement. The factors governing bone ingrowth, stress shielding and clinical results*, J. Bone Joint Surg. Br., 1987, 69, 45–55.

[10] FLOERKEMEIER T., WELTIN J., BUDDE S., HURSCHLER C., WINDHAGEN H., Von LEWINSKI G., GRONEWOLD J., *A short stem with metaphyseal anchorage reveals a more physiological strain pattern compared to a standard stem : an experimental study in cadavaric bone*, Acta Bioeng. Biomech., 2019, 21 (2), 153–159.

[11] HEINER A.D., *Structural properties of fourth-generation composite femurs and tibias*, J. Biomech., 2008, 41, 3282–3284.

[12] HEINER A.D., BROWN T.D., *Structural properties of a new design of composite replicate femurs and tibias*, J. Biomech., 2001, 34, 773–781.

[13] HERRERA A., PANISELLO J.J., IBARZ E., CEGONINO J., PUERTOLAS J.A., GRACIA L., *Long-term study of bone remodelling after femoral stem: a comparison between dexa and finite element simulation*, J. Biomech., 2007, 40, 3615–3625.

[14] HERRERA A., REBOLLO S., IBARZ E., MATEO J., GABARRE S., GRACIA L., *Mid-term study of bone remodeling after femoral cemented stem implantation: comparison between DXA and finite element simulation*, J. Arthroplasty, 2014, 29, 90–100.

[15] HUISKES R., WEINANS H., DALSTRA M., *Adaptive bone remodeling and biomechanical design considerations for noncemented total hip arthroplasty*, Orthopedics, 1989, 12, 1255–1267.

[16] HYODO K., INOMOTO M., MA W., MIYAKAWA S., TATEISHI T., *Thermoelastic femoral stress imaging for experimental evaluation of hip prosthesis design*, JSME Int. J. Ser. C. Mech. Sys., Machine Elements and Manuf, 2001, 44, 1065–1071.

[17] KEYAK J.H., ROSSI S.A., JONES K.A., SKINNER H.B., *Prediction of femoral fracture load using automated finite element modeling*, J. Biomech., 1998, 31, 125–133.

[18] KIM Y.H., KIM J.S., CHO S.H., *Strain distribution in the proximal human femur. An in vitro comparison in the intact femur and after insertion of reference and experimental femoral stems*, J. Bone Joint Surg. Br., 2001, 83, 295–301.

[19] MCNAMARA B.P., CRISTOFOLINI L., TONI A., TAYLOR D., *Relationship between bone-prosthesis bonding and load transfer in total hip reconstruction*, J. Biomech., 1997, 30, 621–630.

[20] NISHINO T., MISHIMA H., KAWAMURA H., SHIMIZU Y., MIYAKAWA S., OCHIAI N., *Follow-up results of 10–12 years after total hip arthroplasty using cementless tapered stem – frequency of severe stress shielding with synergy stem in Japanese patients*, J. Arthroplasty, 2013, 28, 1736–1740.

[21] OBA M., INABA Y., KOBAYASHI N., IKE H., TEZUKA T., SAITO T., *Effect of femoral canal shape on mechanical stress distribution and adaptive bone remodelling around a cementless tapered-wedge stem*, Bone Joint Res., 2016, 5, 362–369.

[22] OKAZAKI Y., ISHII D., OGAWA A., *Spatial stress distribution analysis by thermoelastic stress measurement and evaluation of effect of stress concentration on durability of various orthopedic implant devices*, Mater. Sci. Eng. C., 2017, 75, 34–42.

[23] OTANI T., WHITESIDE L.A., WHITE S.E., *The effect of axial and torsional loading on strain distribution in the proximal femur as related to cementless total hip arthroplasty*, Clin. Orthop. Relat. Res., 1993, 292, 376–383.

[24] PIVEC R., JOHNSON A.J., MEARS S.C., MONT M.A., *Hip arthroplasty*, The Lancet, 2012, 380, 1768–1777.

[25] Registry, A.O.A.N.J.R. Hip, Knee & Shoulder Arthroplasty: 2020 annual report. Adelaide: AOA 2020. https://aoanjrr.sahmri.com/annual-reports-2020.

[26] SPEIRS A.D., HELLER M.O., TAYLOR W.R., DUDA G.N., PERKA C., *Influence of changes in stem positioning on femo-*

ral loading after THR using a short-stemmed hip implant, Clin. Biomech. (Bristol, Avon), 2007, 22, 431–439.

[27] TAKEHASHI H., NISHINO T., MISHIMA H., WADA H., YAMAZAKI M., HYODO K., *Stress distribution of cementless stems with unique flanges in a rectangular cross-section: thermoelastic stress imaging study*, J. Rural Med., 2021, 16, 83–90.

[28] The National Joint Registry 17th Annual Report 2020. London: National Joint Registry 2020, https://www.njrcenter.org.uk

[29] THOMSON W., On the Dynamical Theory of Heat, with numerical results deduced from Mr Joule's Equivalent of a Thermal Unit, and M. Regnault's Observations on Steam, Trans. R. Soc. Edinburgh, 1853, 20, 261–288.

[30] VIDALAIN J.P., *Twenty-year results of the cementless Corail stem*, Int. Orthop., 2011, 35, 189–194.

[31] WILLBURGER R.E., HEUKAMP M., LINDENLAUB P., EFE T., PETERLEIN C.D., SCHUTTLER K.F., *Excellent midterm survival and functional outcomes of a fully hydroxyapatite-coated cementless stem: first results of a prospective multicenter study*, Arthroplast Today, 2020, 6, 201–205.